In-Flight Boundary-Layer Transition on a Large Flat Plate at Supersonic Speeds

D.W. Banks, M. A. Frederick
Dryden Flight Research Center, Edwards, California

R.R. Tracy, J.R. Matisheck, N.D. Vanecek
Aerion Corporation, Reno, Nevada

NASA STI Program ... in Profile

Since its founding, NASA has been dedicated to the advancement of aeronautics and space science. The NASA scientific and technical information (STI) program plays a key part in helping NASA maintain this important role.

The NASA STI program operates under the auspices of the Agency Chief Information Officer. It collects, organizes, provides for archiving, and disseminates NASA's STI. The NASA STI program provides access to the NASA Aeronautics and Space Database and its public interface, the NASA Technical Reports Server, thus providing one of the largest collections of aeronautical and space science STI in the world. Results are published in both non-NASA channels and by NASA in the NASA STI Report Series, which includes the following report types:

- TECHNICAL PUBLICATION. Reports of completed research or a major significant phase of research that present the results of NASA Programs and include extensive data or theoretical analysis. Includes compila-tions of significant scientific and technical data and information deemed to be of continuing reference value. NASA counter-part of peer-reviewed formal professional papers but has less stringent limitations on manuscript length and extent of graphic presentations.

- TECHNICAL MEMORANDUM. Scientific and technical findings that are preliminary or of specialized interest, e.g., quick release reports, working papers, and bibliographies that contain minimal annotation. Does not contain extensive analysis.

- CONTRACTOR REPORT. Scientific and technical findings by NASA-sponsored contractors and grantees.
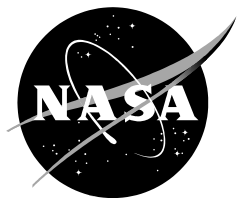
- CONFERENCE PUBLICATION. Collected papers from scientific and technical conferences, symposia, seminars, or other meetings sponsored or co-sponsored by NASA.

- SPECIAL PUBLICATION. Scientific, technical, or historical information from NASA programs, projects, and missions, often concerned with subjects having substantial public interest.

- TECHNICAL TRANSLATION. English-language translations of foreign scientific and technical material pertinent to NASA's mission.

Specialized services also include organizing and publishing research results, distributing specialized research announcements and feeds, providing information desk and personal search support, and enabling data exchange services.

For more information about the NASA STI program, see the following:

- Access the NASA STI program home page at http://www.sti.nasa.gov

- E-mail your question to help@sti.nasa.gov

- Fax your question to the NASA STI Information Desk at 443-757-5803

- Phone the NASA STI Information Desk at 443-757-5802

- Write to:
  STI Information Desk
  NASA Center for AeroSpace Information
  7115 Standard Drive
  Hanover, MD 21076-1320

In-Flight Boundary-Layer Transition on a Large Flat Plate at Supersonic Speeds

D.W. Banks, M. A. Frederick
Dryden Flight Research Center, Edwards, California

R.R. Tracy, J.R. Matisheck, N.D. Vanecek
Aerion Corporation, Reno, Nevada

Abstract

A flight experiment was conducted to investigate the pressure distribution, local-flow conditions, and boundary-layer transition characteristics on a large flat plate in flight at supersonic speeds up to Mach 2.00. The tests used a NASA testbed aircraft with a bottom centerline mounted test fixture. The primary objective of the test was to characterize the local flow field in preparation for future tests of a high Reynolds number natural laminar flow test article. A second objective was to determine the boundary-layer transition characteristics on the flat plate and the effectiveness of using a simplified surface coating. Boundary-layer transition was captured in both analog and digital formats using an onboard infrared imaging system. Surface pressures were measured on the surface of the flat plate. Flow field measurements near the leading edge of the test fixture revealed the local flow characteristics including downwash, sidewash, and local Mach number. Results also indicated that the simplified surface coating did not provide sufficient insulation from the metallic structure, which likely had a substantial effect on boundary-layer transition compared with that of an adiabatic surface. Cold wall conditions were predominant during the acceleration to maximum Mach number, and warm wall conditions were evident during the subsequent deceleration.

Nomenclature

CF	cross flow (transition mechanism)
CLIP	Centerline Instrumented Pylon
C_P	pressure coefficient
IR	infrared
M	Mach number
M_{inf}	freestream Mach number
N	log of the disturbance amplitude ratio from the point of neutral stability to the point of transition (also N-factor)
NASA	National Aeronautics and Space Administration
NLF	natural laminar flow
SBLT	Supersonic Boundary Layer Transition (project)
SSNLF	Supersonic Natural Laminar Flow (project)
TS	Tollmien-Schlichting (transition mechanism)
α	angle of attack, deg
β	angle of sideslip, deg

Introduction

Supersonic cruise aircraft suffer from limited range and high costs, as well as poor subsonic flight characteristics compared to aircraft designed to cruise at high subsonic speed. The primary reason for the former is the reduced aerodynamic efficiency (lift-to-drag ratio) caused by the addition of wave drag at supersonic speed, and the latter is because highly swept supersonic lifting surfaces typically have poor subsonic and low-speed aerodynamic characteristics. Careful configuration design (refs.1 and 2) can, however, reduce but not eliminate supersonic wave drag. Also, laminar boundary layers are much more stable at supersonic speeds as compared to high subsonic speeds, and the resulting reduction in skin friction drag offers a means of offsetting some of the wave drag penalties. In addition, the wing shapes required to support extensive natural laminar flow do not incorporate significant sweep and thus can provide improved subsonic cruise efficiency as well as better takeoff and landing characteristics. Better understanding of transition at supersonic speeds will enable improved design methodology and transition prediction.

System studies of applications of supersonic natural laminar flow have been performed and show sufficient improvement in aerodynamic efficiency, thus significantly benefiting range and economics comparable to subsonic aircraft in the same role.

In view of the large effect of laminar flow on aerodynamic efficiency, accurate prediction of the onset of boundary-layer transition is critical to the successful design of laminar flow aircraft. Many factors influence the stability of the laminar boundary layer and, hence, transition. These factors include Mach number, Reynolds number, pressure distribution, wing sweep, surface roughness and waviness, free-stream turbulence, acoustic disturbances, and wall temperature. For most modern airframes, transition is governed by attachment-line contamination, cross-flow (CF) instability, Tollmien-Schlichting (TS) instability, laminar separation, or a combination of these factors. Growth of TS instabilities in the laminar boundary layer tends to be the dominant source of transition onset on smooth wings with little or no sweep at high Reynolds numbers. Growth of CF instabilities tends to be the dominant source on wings with leading-edge sweep angles exceeding approximately 20° with modest leading-edge radii. Attachment-line contamination (spanwise flow along a leading edge with sufficient thickness can cause instabilities and transition) can occur on swept wings with larger leading-edge radii.

Extensive theoretical work has been performed in the area of boundary-layer stability, resulting in several codes such as LASTRAC (refs. 3 and 4) that solve for disturbance growth in compressible three-dimensional boundary layers. Transition prediction typically involves assuming a value of "N," the logarithm of the disturbance amplitude ratio from the point of neutral stability to the point of transition (ref. 5). This value is estimated by experiment with similar geometry and flow conditions.

There has been a substantial effort in the area of active laminar flow control, typically using suction to delay transition, both at subsonic and supersonic speeds (refs. 6 and 7). Efforts at supersonic speeds have been motivated by the inability of a highly swept supersonic wing to support natural laminar flow because of attachment-line contamination and the high levels of cross flow near the leading edge. These efforts have included both theoretical studies and flight tests, more recent flight tests being the National Aeronautics and Space Administration (NASA) F-16 (General Dynamics, now Lockheed Martin, Bethesda, Maryland) F-16XL Laminar Flow Research Aircraft tests. The F-16XL tests had limited success and entailed complex wing structures and pumping equipment with cost, weight, and maintenance impacts in application. The natural laminar flow (NLF) approach avoids most of these drawbacks and thus has appeal from the systems perspective.

The public literature contains flight data supporting an N-value of 9 or 10 for conical bodies at supersonic speeds, but contains little or no flight data for planar surfaces with pressure gradients. Supersonic wind tunnels have turbulent wall boundary layers with high disturbance levels and thus cause earlier transition than what is seen in flight. A Mach 3.5 "quiet tunnel" was developed at the NASA Langley Research Center (Hampton, Virginia) in the 1980s; one test of a flat plate at adiabatic conditions was reported that supports an N-value of 10 (refs. 8-10).

There is thus a need for transition data on planar surfaces with chord-wise and cross-flow pressure gradients and over a range of Mach numbers and wall temperature ratios, in order to confirm the transition levels predicted by stability theory. In addition to pressure gradients and cooling, there are other transition factors that have received limited study in the context of subsonic wings and axi-symmetric bodies at hypersonic speeds, but not for supersonic wing shapes. These factors also require flight tests and include the effects on supersonic transition of radiated noise, surface roughness, and leading-edge bluntness.

Airfoil designs capable of maintaining significant runs of natural laminar flow at low supersonic speeds (Mach up to ~2.0) have been shown by theoretical and empirical means and recently demonstrated at moderate Reynolds numbers (~10^7) in flight. Most prior flight-validated supersonic laminar flow techniques relied on active boundary-layer control at least near the leading edge. A more recent design philosophy utilizes low leading-edge sweep to reduce growth of cross-flow instabilities in the boundary layer and relatively thin wing sections to subsequently minimize wave drag. These limited flight results and other ground tests at low to moderate Reynolds numbers have verified the concept. Other methods have been proposed that reduce supersonic viscous drag. Flight data at high chord Reynolds numbers are

required to prove any design concept prior to implementation on full-scale aircraft. These types of tests would also provide data to validate design tools and turbulence models.

Boundary-layer stability theory indicates that extensive laminar flow can be maintained on aircraft wings and other surfaces at supersonic speeds by appropriate configuration design. There are limited suitable experimental transition data available, however, for verification of the theory for planar surfaces with pressure gradients. The major benefit of this technology is that it is passive in nature. There has been a significant amount of computational analyses and systems studies of proposed configurations that employed such a system. The system appears to offer the best trades at the business jet class of aircraft.

Aerion Corporation (Reno, Nevada) has a patented design for an efficient supersonic business jet based on maintaining large runs of laminar flow (up to 70%) on its lifting surfaces. Prior and current supersonic cruise aircraft likely have no significant laminar flow on any surfaces. The Aerion design employs a relatively unswept wing to effectively eliminate cross flow, a major boundary-layer transition mechanism. The modified bi-convex wing maintains a favorable pressure gradient from leading to trailing edge supersonically, and is relatively thin to minimize wave drag. The Aerion design reduces total airframe drag by up to 20% over conventional swept wing designs such as the Concorde (manufactured under the combined efforts of Aerospatiale [France] and the British Aircraft Corporation [United Kingdom]). The Aerion design also maintains efficient performance at subsonic speeds, allowing a mixed supersonic/subsonic cruise profile and thus missions with both segments of supersonic speeds over oceans and segments of high subsonic speeds over land where supersonic flight is restricted. Aerion Corporation plans to obtain flight data supporting the physics of their concept and the sensitivity of laminar flow to surface roughness and imperfections.

The National Aeronautics and Space Administration has an interest in reducing the barriers to efficient supersonic flight and has teamed with Aerion Corporation to explore the physics of high Reynolds number boundary-layer transition. Joint flight tests between NASA and Aerion have been conducted since 1999. To date, these tests have employed a NASA F-15B (McDonnell Douglas, now The Boeing Company, Chicago, Illinois) testbed aircraft (discussed in detail below) with a bottom mounted test article as shown in figure 1. Figure 2 shows a typical installation with the test article, the Centerline Instrumented Pylon (CLIP), and infrared (IR) camera pod. This method allows testing of large-scale test articles at Reynolds numbers similar to full-scale flight conditions.

Previous flight test results have demonstrated the feasibility of maintaining supersonic natural laminar flow with the low-sweep concept (Supersonic Natural Laminar Flow project or SSNLF, Phase I & II tests, 1999 to 2002) (refs.11 and 12). Figure 3 shows the SSNLF test article mounted to the NASA F-15B testbed aircraft. Figure 4 shows the initial IR image results showing supersonic natural laminar flow at a freestream Mach number of ~1.8. These low-sweep results, however, were limited in Reynolds number to approximately 10 million. The primary objective of the SSNLF project was to validate the predictions and ground test results of maintaining supersonic natural laminar flow at moderate Reynolds numbers. A follow-on program, named Supersonic Boundary Layer Transition (SBLT), has the objective of expanding on the results of the SSNLF project by increasing the Reynolds number and testing more complex lifting surfaces. The SBLT investigation will use larger scale test articles and a multi-purpose support structure to perform supersonic natural laminar flow (NLF) testing at significantly larger chord Reynolds numbers. The first phase of the SBLT investigation was to better define the flow field in the vicinity of the test article on the F-15B testbed aircraft. This objective was accomplished by using a flat plate test article with an array of surface pressures and using five 5-hole probes near the leading edge of the flat plate to define the immediate upstream flow. The test article backside indicating the flow probes is shown in figure 5(a) and the surface pressure array is shown in figure 5(b). The test article is discussed in more detail in the following section. This calibration test article had a simplified surface coating in lieu of surface insulation. More surface insulation would likely be necessary to obtain a near adiabatic test surface in the given environment. Nonetheless, IR thermography was used to observe the boundary-layer transition on the flat plate during this investigation.

The SBLT phase 1 test article (flat plate) was exposed to large variations in temperature, which without properly insulating the surface would likely have a significant effect on the stability of the boundary layer and consequently the transition location. Cold wall conditions are known to be stabilizing to air boundary layers at low supersonic Mach numbers (M<3.00) where the Tollmien-Schlichting (TS) first mode transition dominates (ref. 13). Warm wall conditions are conversely destabilizing. A qualitative study of the effect of the wall temperature on boundary-layer transition was conducted with the IR thermography results from SBLT phase 1. The characteristics of flat plates, including transition (ref. 14), are well documented. The results from this test will aid in the design of the phase 2 supersonic NLF test article.

Methodology and Approach

A digital IR imaging system was packaged within a specially designed pod and mounted on the right-hand armament rail (under the engine inlet) on an F-15B aircraft (fig. 2). The camera utilizes an Indium Antimonide (InSb) focal plane with 640 X 512 pixels, with 20-micron pitch. The sensor responds in the 3-5 micron spectral range. A 13-mm lens was selected to capture a complete view of the experiment with minimal background within the field of view.

To minimize the size of the camera pod and resultant drag, the sensor was oriented parallel to the airflow. This orientation also placed the line of sight parallel to the experiment. A prism was incorporated in the design to fold the line of sight inboard and down to center on the region of interest. A silicon window with an antireflection coating optimized for the 3-5 micron spectral band was installed on the inner surface of the pod directly in front of the prism. The camera provided simultaneous analog (RS-170) and 14-bit digital output (high-speed serial interface).

Data are currently collected on HI-8 (8-mm) videotape for the analog output and to a digital recorder for the digital output. The recording system will support continuous collection of 14-bit digital data for up to approximately two hours. Digital data collection can be started and stopped using a cockpit control switch.

The NASA F-15B test aircraft is a two-seat version of the F-15A aicraft: a high performance, supersonic, all-weather air-superiority fighter built by McDonnell-Douglas Aircraft Company (now The Boeing Company). Two Pratt & Whitney (East Hartford, Connecticut) F100-PW-100 afterburning turbofan engines power the F-15B aircraft. The F-15B aircraft (ref. 15) is 63.75 ft (19.43 m) long with a wingspan of 42.8 ft (13.05 m) and a basic takeoff weight (interceptor configuration) of 41,500 lb (18,824 kg). The test article was mounted on the centerline tank location on a specially modified pylon. The aircraft is outfitted with a flight test nose boom in order to obtain accurate air data during flight.

The test article was fabricated mostly of 6061 Aluminum. Structurally it consisted of two major pieces: the test surface and a main structural piece called the "strongback." The test surface was attached to the side of the strongback, which in turn was connected to the specially modified centerline pylon, which provided attachment to the aircraft. The pylon is a modified external tank pylon that has the fuel mechanisms removed to allow room for instrumentation and has a large splitter plate on the bottom, which shields the test article from the turbulent flow under the aircraft. This modified pylon is called the Centerline Instrumented Pylon or CLIP and can be seen in figure 2. As mentioned above, the test surface had a simplified surface coating, which did not provide adequate insulation from the underlying metallic structure (to be near adiabatic). This condition was known to be a possibility from the beginning of the test phase, but the primary objective of this phase of testing was to define the flow field at the test location in preparation for future laminar flow test articles. The gathering of IR data to observe the transition characteristics of the flat plate remained a secondary objective. The size of the test surface was 84 inches (213.4 cm) long (chordwise direction) and 40.875 inches (103.8 cm) high (spanwise direction), and 0.75 inches (1.9 cm) maximum thickness, with a 10° swept leading edge.

Six 5-hole probes were used during this investigation in order to define the local flow field. Five of these probes were located near the leading edge of the test article and one was located on the apex of the pylon splitter plate; see figure 5(a). The probes are placed adjacent to the leading edge of the flat plat such

that the shocks from the probes will impact the non-measuring side behind the leading edge and not contaminate the measurements. Also, the shocks from the leading edge of the flat plate will cross the probes behind the pressure ports at the test conditions (M≥1.40). The local flow has been processed through several major shock waves and expansions and is not expected to match freestream values. The major effect is a local flow angularity. This local flow angularity typically consists of a downward component and a port to starboard sideflow component. The downward component has the effect of increasing the effective sweep angle on the test article. The sideflow has the effect of putting the flat plate at a slightly positive angle of attack.

Significant local-flow distortions are observed at low Mach numbers and consequently the centerline pylon area is not considered useable for testing much below M=1.40. The flight profile typically consisted of level supersonic accelerations up to M=2.00 and then level decelerations. The altitude was maintained at a near constant value. During the accelerations the engine was set in a high afterburning setting; during the decelerations the engine power was maintained at a maximum non-afterburning setting. The inlet flow is known to be the same at maximum non-afterburning and afterburning power settings for a given set of flight and atmospheric conditions. The inlet flow field, namely inlet spillage, can have significant effects on the local field under the aircraft at the test location. This inlet effect and identical flight and atmospheric conditions result in the local flow field at the test location being same at both power settings during the level acceleration/deceleration maneuver. The flight profile consisted of climbs to altitude of approximately 40,000 to 42,000 ft (12,200 to 12,800 m) and a cruise to the end of the supersonic test range. This cruise was typically of 10 to 15 minutes and caused the test article and structure to cold soak at temperatures of -70° to -100°F (-57° to -73°C). The subsequent supersonic acceleration created aerodynamic heating up to approximately +240°F (+116°C) at M=2.00. At lower supersonic Mach numbers the test article realized a substantial (though not measured) difference in surface temperature between the acceleration and deceleration portion of the supersonic maneuver. Significant differences in the measured transition location were observed for these pairs of test points that had no significant differences in condition except for the surface temperature. Thus, the inference can be made that these changes in transition were due to the wall temperature differences.

Surface pressure data, local flow data, and analog IR data were captured during the entire flight. Figure 6(a) shows sample analog IR results at M=1.57 during the acceleration; figure 6(b) shows the local pressure coefficient (C_p) and leading-edge flow angles (α and β) also for M=1.57 during the acceleration. Figures 6(c) and 6(d) show the IR image, and C_p contours with flow angles for the deceleration, respectively for M=1.57. The C_p contour plots were processed using the in-flight pressure data on the flat plate. Figures 7(a) and 7(b) show the IR and C_p with flow angle results for the M=2.00 condition. The pressure contours for the acceleration and deceleration parts of the maneuver at a given Mach number, such as that shown in figures 6(b) and 6(d) for M=1.57, are virtually identical. Also, the inflow angles are very close, indicating that the assumption of similar flow conditions for the same Mach number during the acceleration and deceleration is valid. Again, the only significant difference between these two test points (at the same Mach number) is the surface or wall temperature. The analog IR data show the relatively cooler areas as darker shades of gray and the warmer areas as lighter shades. The transition zone is indicated on the figure, as is a shock wave that affects transition at lower Mach numbers. The shock wave is evident near the end of the transition zone. The analog images are automatically adjusted, which provides better-looking images, but the raw intensity values are obscured by this automatic processing, subsequently eliminating quantitative analysis. The transition zone is clearly seen as the darker area on the first 25% of the chord for M=1.57 and much closer to the leading edge for M=2.00. The zone is terminated by turbulent wedges, where critical roughness quickly changes the boundary layer to turbulent and propagates as a wedge downstream. These areas are darker because laminar boundary layers allow less heat to be transferred from the freestream to the surface (colder than freestream) than do turbulent boundary layers, thus having a colder surface beneath the laminar boundary layers than the turbulent ones. Some of the apparent features seen aft on the test surface are due to reflections from the very smooth surface. The reflections cease as the test article warms, such as at M=2.00 in figure 7(a), at

which point the emitted energy is much greater than the reflected energy. Also, the position of the camera and optics relative to the test article causes some geometric distortion in the acquired images.

Digital IR data (30 frames per second) were captured during the entire supersonic portion of the flight. The digital images were processed by performing a histogram equalization and then applying a suitable color mapping. The color mapping used is shown in figures 8(a) and 8(b). Figures 8(a) and 8(b) show sample digital images (M=1.65) from the acceleration and deceleration maneuver phases, respectively. The transition zone and shock wave impingement are also indicated. This method optimizes each image for contrast to better visualize the flow phenomena but results in a different color versus temperature (intensity) between images. Future tests will incorporate temperature sensing devices at key locations that should allow a calibration of the pixel intensity level to a temperature. This will provide a means of measuring the entire surface temperature profile and quantitatively analyzing the wall temperature effects. Additionally, development of algorithms to fix the geometric distortions has been initiated. The results of this current analysis are presented with the color mapped digital images.

Results and Discussion

Data are presented for freestream Mach numbers of 1.40, 1.50, 1.60, 1.70, 1.80, and 1.85 and are shown in figures 9(a) to 14(b). These data were obtained during a single flight maneuver. The data are presented as paired images for each Mach number, one during the acceleration (a) and one during the deceleration (b). As previously discussed, the test article was cold soaked prior to the initiation of the supersonic run. This means that during the acceleration phase the test surface wall was colder than that of an adiabatic wall; however, the test article surface temperature was expected to rise during the acceleration. Subsequently, during much of the deceleration the surface temperature was assumed to be warmer than that of an adiabatic wall. In any case, the surface temperature during the deceleration phase would be warmer than that for the acceleration phase. The leading edge should heat faster than the rest of the test article due to the higher aerodynamic heating and less thermal mass. There is likely a single condition where the wall temperature, at least near the leading edge, is close to or matches the adiabatic condition. No quantitative temperature measurements were obtained during this test; therefore, the wall temperature departure from adiabatic is assumed based on the flight test profile, although some qualitative values can be inferred from the raw IR intensities that were recorded.

The laminar flow regions are noticed as a sharp change in the coloring, usually accompanied by "wedging" (turbulent flow propagating as a wedge from critical disturbances). The coated surface also has some noticeable amount of reflectivity, which is usually overshadowed by the temperature effects and is only evident at the lower Mach numbers during the acceleration portion of the maneuver due to the surface being made very smooth. This effect will be minimized during the subsequent laminar flow test but cannot be entirely eliminated due to the desire for a relatively smooth surface. There is also some indication of the subsurface pressure plumbing; these show up as small round areas under the pressure ports and chordwise lines where the tubing is laid.

A noticeable and important feature, that of a shock wave impingement, is observed in most of the images. It is much more noticeable in movies made from these obtained images at 30 frames per second. The shock wave is responsible for terminating the laminar flow at the lower Mach number acceleration conditions (M≤1.40). The shock appears near the terminus of the M=1.50 (fig. 7(a)) cold wall transition zone. At higher Mach numbers the shock moves aft, located approximately mid-chord at M=1.60 (figs. 11(a) and (b)) and within 20% of the trailing edge at M=1.85 (figs. 14(a) and (b)). Notice the shock locations are nearly the same for both the acceleration and deceleration phases at the same Mach number. This is expected since the upstream flow conditions should be nearly identical except for minor aircraft excursions. For all Mach numbers the deceleration phase results show much less laminar flow and earlier transition than for the acceleration phase. At M=1.40 (figs. 9(a) and (b)) the transition is dominated by the shock wave and shows a smaller difference between the two. At M=1.50 (fig. 10(a)) the amount of laminar flow seen during the acceleration appears to be the maximum even though it subsequently is terminated by the shock. At M=1.60, 1.70, and 1.80 (figs. 11(a), 12(a), and 13(a), respectively) the overall

transition boundary moves slightly forward with increasing Mach number, but the more noticeable effect is that the outboard flow (near the bottom) moves forward much more quickly, possibly because of some cross-flow contamination [the fine sawtooth pattern seen at M=1.80 (fig. 13(a)) and 1.85 (fig. 14(a))] and the disturbance coming off the outboard leading-edge corner.

The IR false color images show relative temperature for each individual image. The progression of time (acceleration to deceleration) shows the edges of the test article warming significantly compared to the central portion. This is due to the aerodynamic heating being more effective on the parts of the test article that are not in direct contact with the structural strongback; also, aerodynamic heating would expected to be more effective near the leading edge than the trailing edge. The strongback constitutes a very large thermal mass, which would obviously take much longer to change temperature. A rectangular area near the trailing edge (~80% chord) that is adjacent to an equipment bay in the strongback indicates warmer temperatures similar to those of the edges. The equipment bay is an open area in the strongback that does not have the thick metallic structure; the area of the test surface over the equipment bay (fig. 5(a)) would not be expected to have the same thermal inertia and should have heating characteristics like the other areas not in contact with the strongback. Additionally, there is some internal heating of this area due to instrumentation and associated temperature control (instrumentation heaters). This indicates that the areas in contact with the strongback are cooler than other areas (the edges, and the area adjacent to the equipment bay). Since each image is separately equalized and processed, the image shows relative temperature distribution of each image, and no quantitative determination regarding the temperature compared to freestream, ambient, or adiabatic can be made. The background behind the test article should remain relatively constant in temperature during the entire maneuver; however, the background color changes significantly during the maneuver. The background color changes from warmer than average (yellow-red) to colder than average (blue). Qualitatively, this indicates that the test article is warming significantly as compared to this background.

The summary of the results of the processed digital images indicates the boundary-layer transition moves significantly forward (earlier) due to wall heating (temperature). As expected, cold wall conditions have a beneficial effect on laminar to turbulent boundary layer transition and warm wall conditions are conversely detrimental.

Summary and Concluding Remarks

A flight experiment was conducted to investigate the pressure distribution, local flow conditions, and boundary-layer transition characteristics on a large flat plate in flight at supersonic speeds up to Mach 2.00. The tests used an F-15B testbed aircraft (McDonnell Douglas, now The Boeing Company, Chicago, Illinois) with a centerline mounted test fixture. The primary objective of the test was to characterize the local flow field in preparation for future tests of a high Reynolds number natural laminar flow test article. A secondary objective was to determine the boundary-layer transition characteristics on the flat plate and the effectiveness of using a simplified surface coating for future laminar flow flight tests employing infrared thermography. Boundary-layer transition was captured using an onboard infrared imaging system. The infrared imagery was captured in both analog and digital formats. Surface pressures were measured with electronically scanned pressure modules connected to 60 surface-mounted pressure orifices. The local flow field was measured with five 5-hole conical probes mounted near the leading edge of the test fixture. Flow-field measurements revealed the local flow characteristics including downwash, sidewash, and local Mach number. Results also indicated that the simplified surface coating did not provide sufficient insulation from the metallic structure, which likely had a substantial affect on boundary-layer transition compared with that of an adiabatic surface. Cold wall conditions were predominant during the acceleration to maximum Mach number, and warm wall conditions were evident during much of the subsequent deceleration. As expected, the cold wall conditions showed significantly more laminar flow and later transition as compared to the warm wall conditions. The infrared imaging system was able to capture shock wave impingement on the surface of the flat plate in addition to indicating laminar-to-turbulent boundary-layer transition.

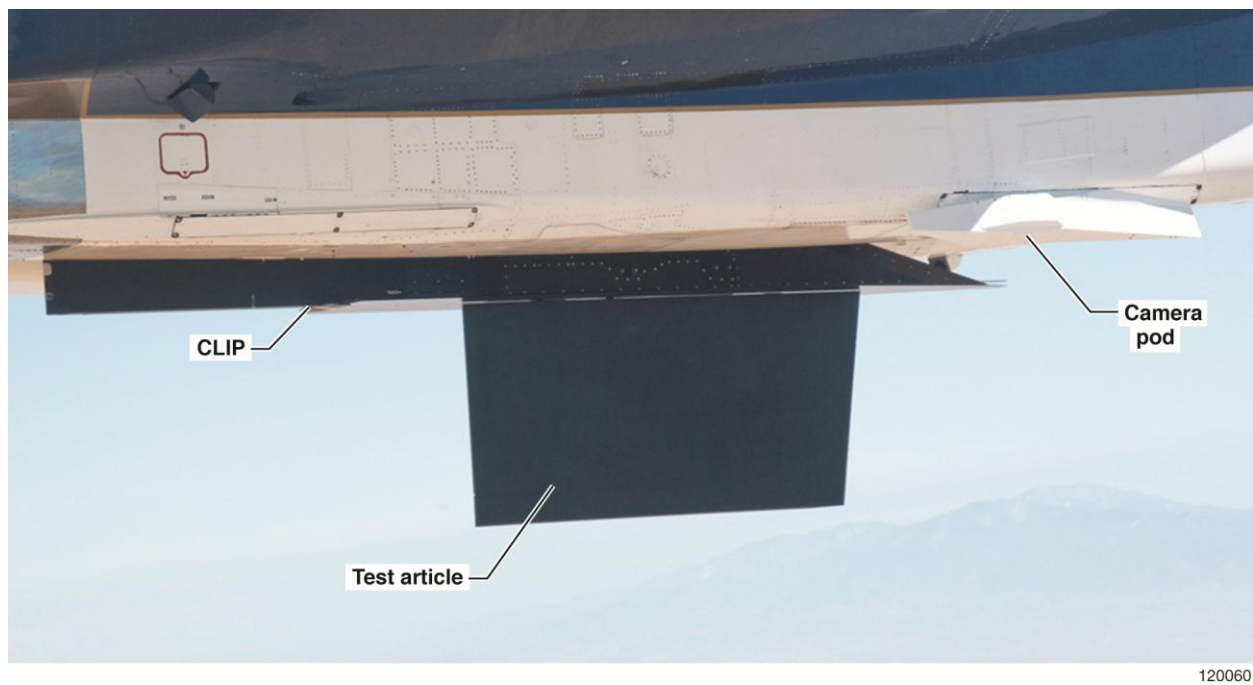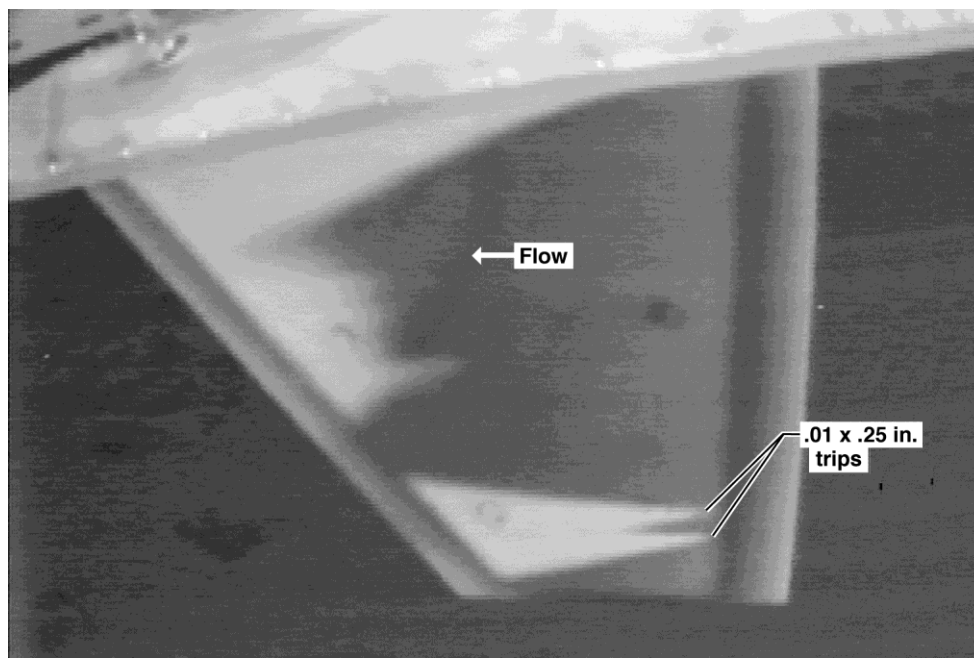# Figures

Figure 1. The NASA F-15B testbed aircraft.

Figure 2. The NASA F-15B testbed aircraft with the infrared camera pod and mounted test article.

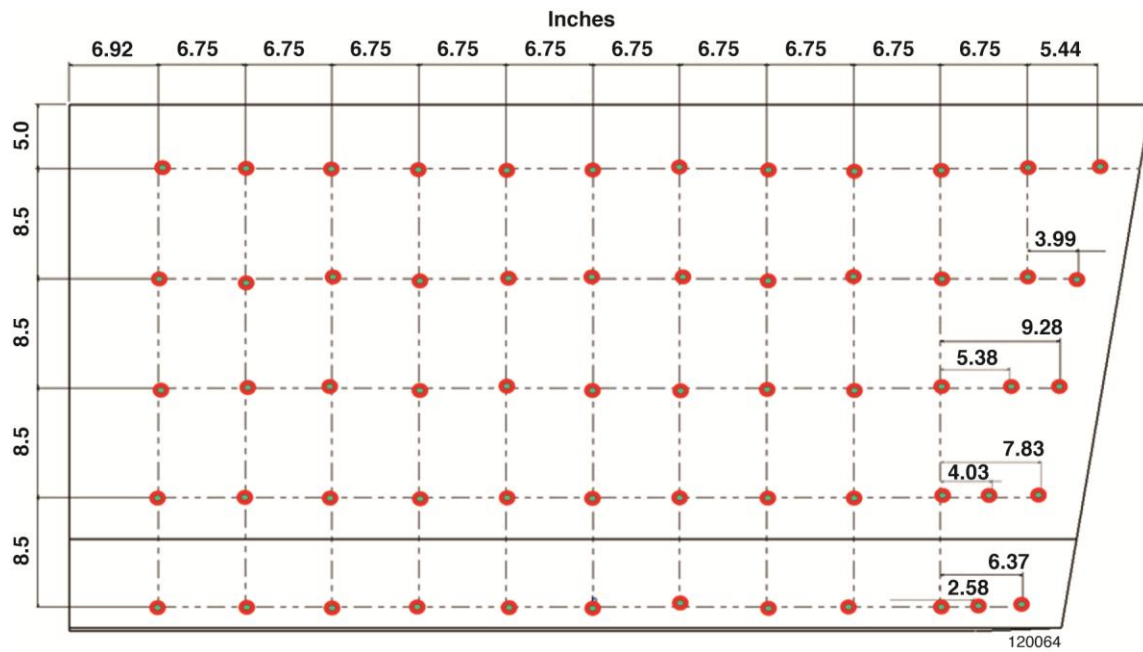Figure 3. The NASA F-15B testbed aircraft with the Supersonic Natural Laminar Flow test article.

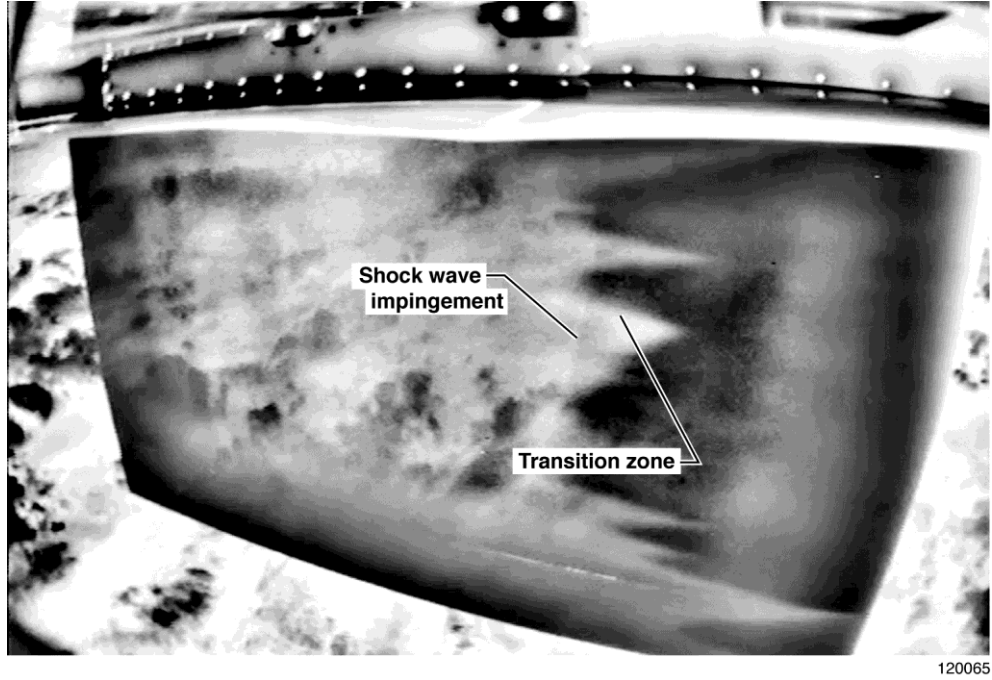Figure 4. Infrared image of the Supersonic Natural Laminar Flow test article showing transition at M~1.80.

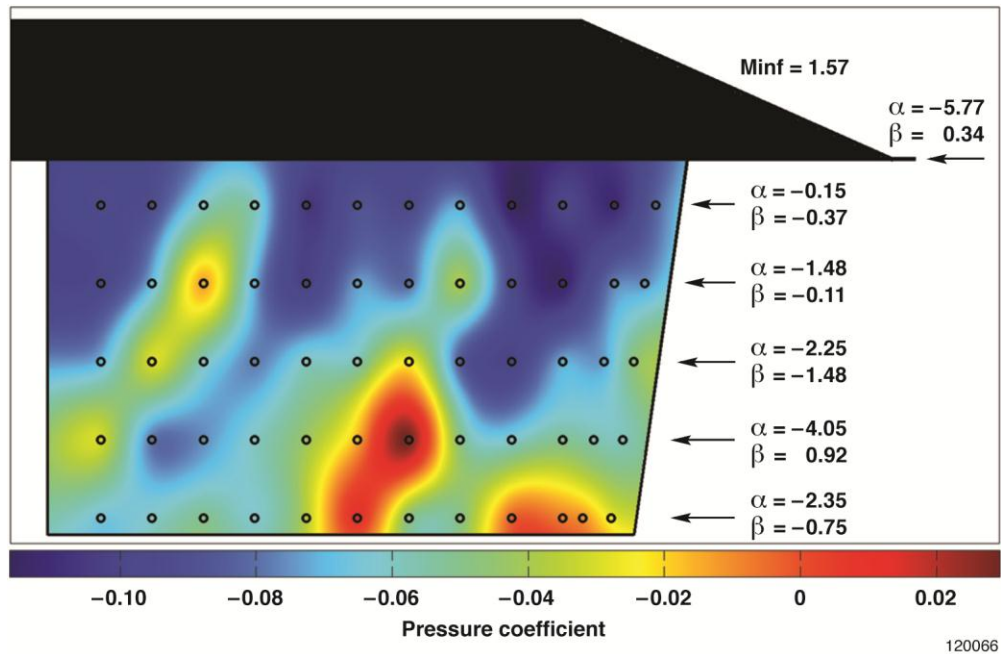(a) Test fixture backside, showing the strongback and local flow measuring probes.

(b) Sketch of test fixture front side showing pressure port locations.

Figure 5. Supersonic Boundary Layer Transition phase 1 test fixture details.

(a) Analog infrared image during acceleration.

(b) Surface pressure coefficients and local flow angles during acceleration.

Figure 6. Analog infrared images, surface pressure distribution, and in-flow angles of Supersonic Boundary Layer Transition phase 1 test fixture at M=1.57.

120067
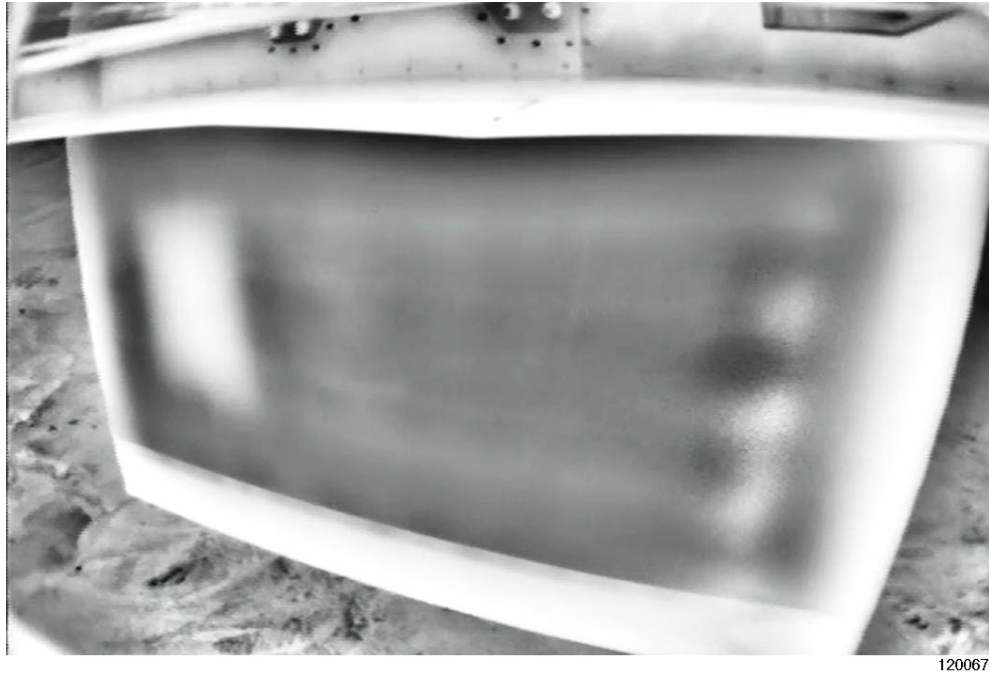
(c) Analog infrared image during deceleration.

Minf = 1.57

$\alpha = -5.60$
$\beta = 0.45$

$\alpha = -0.15$
$\beta = -0.55$

$\alpha = -1.58$
$\beta = -0.42$

$\alpha = -2.36$
$\beta = -1.63$

$\alpha = -4.08$
$\beta = 0.98$

$\alpha = -2.14$
$\beta = -1.05$

−0.10   −0.08   −0.06   −0.04   −0.02   0   0.02
Pressure coefficient

120069
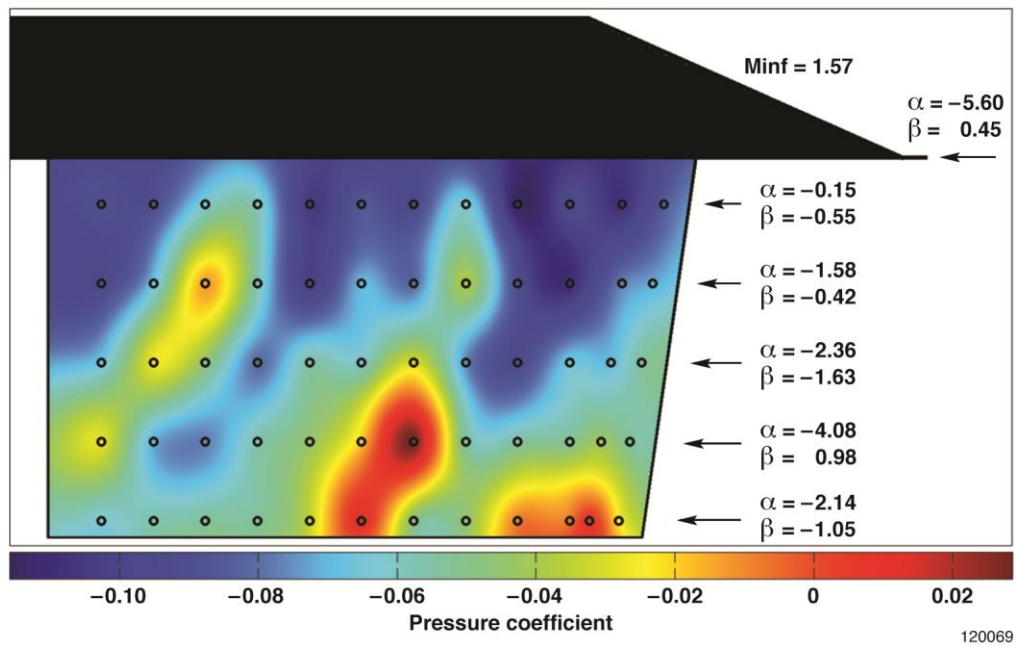
(d) Surface pressure coefficients and local flow angles during deceleration.

Figure 6. Concluded.

12
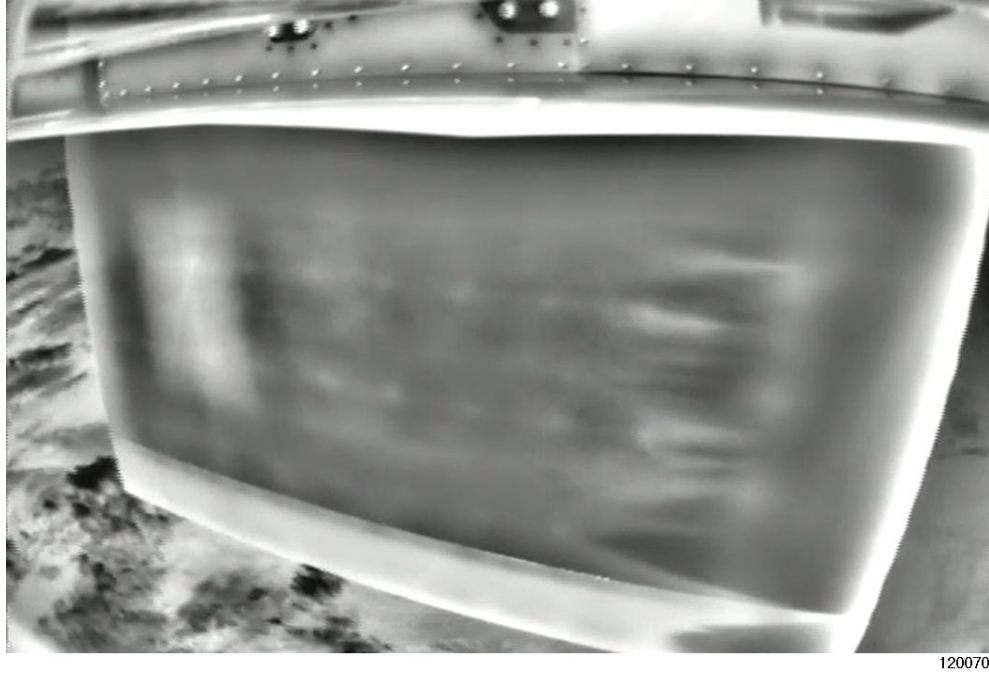
(a) Analog infrared image.
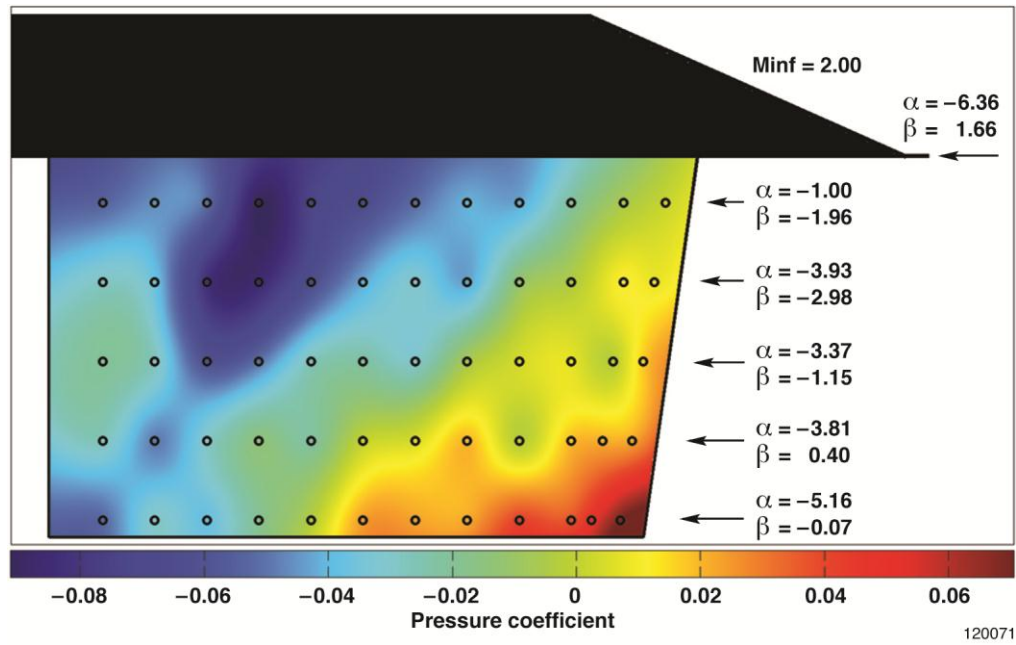
(b) Surface pressure coefficients and local flow angles.

Figure 7. Analog infrared images, surface pressure distribution, and in-flow angles of Supersonic Boundary Layer Transition phase 1 test fixture at a steady M=2.00.
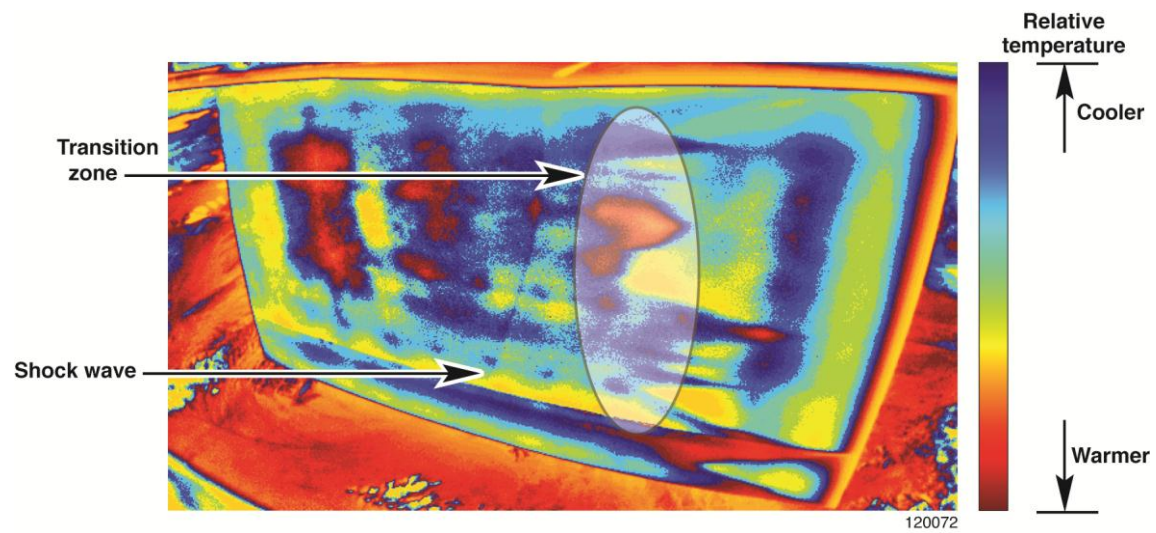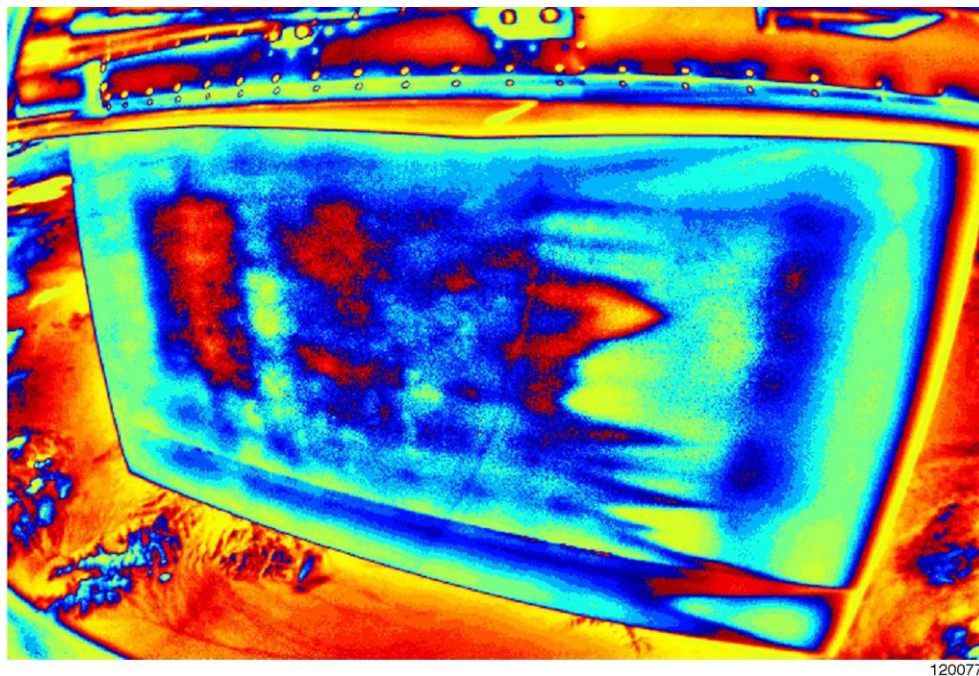
(a) During acceleration.
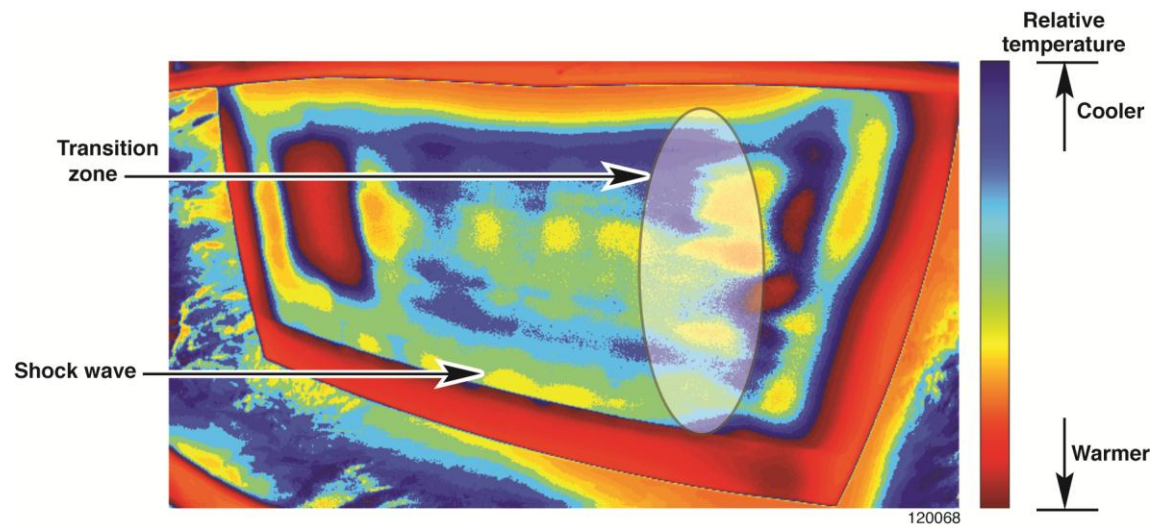
(b) During deceleration.

Figure 8. Processed digital infrared image at M=1.65 showing transition zone, shock wave, and color mapping.
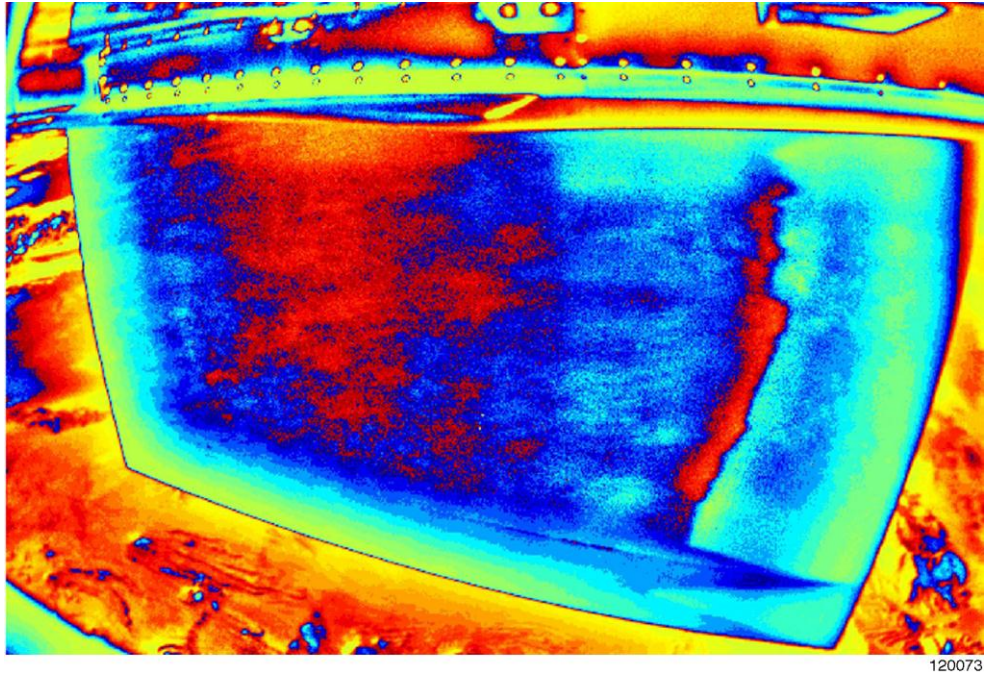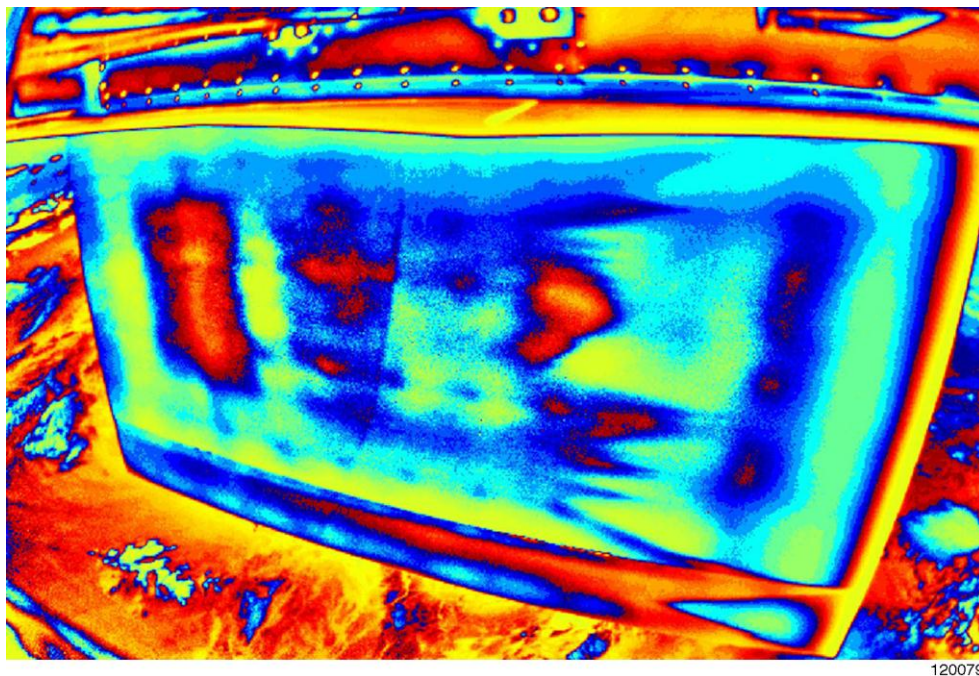
(a) During acceleration.
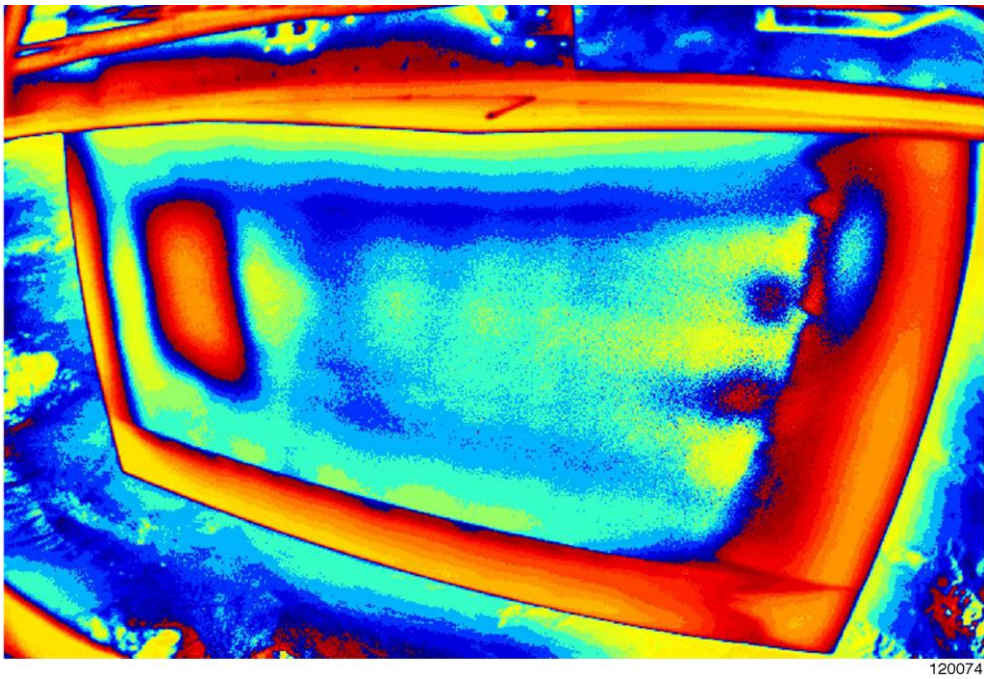
(b) During deceleration.

Figure 9. Processed digital infrared image at M=1.40.
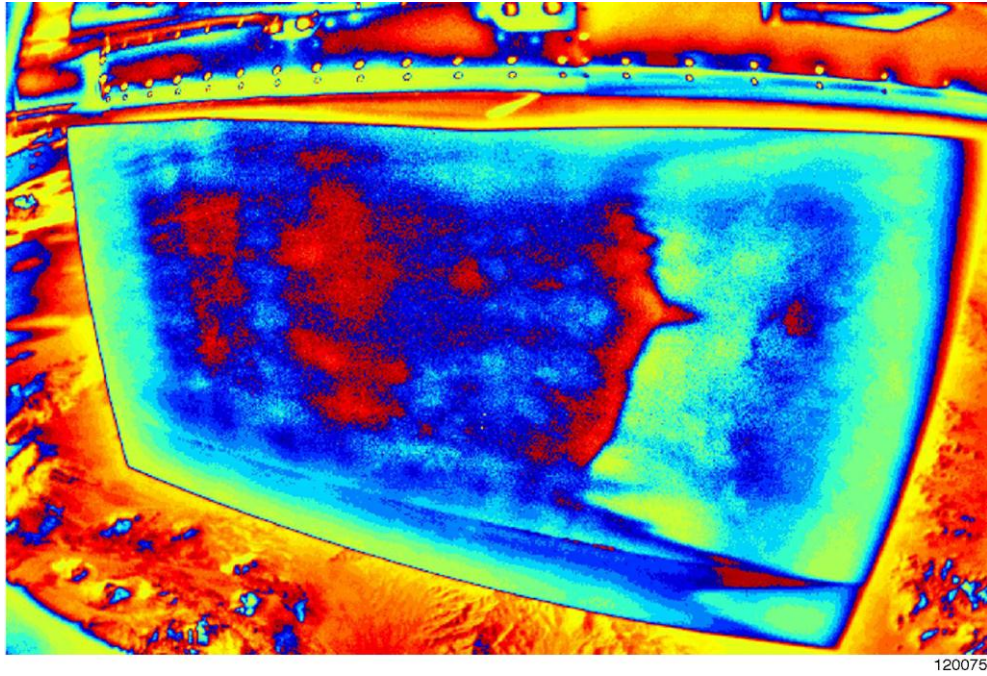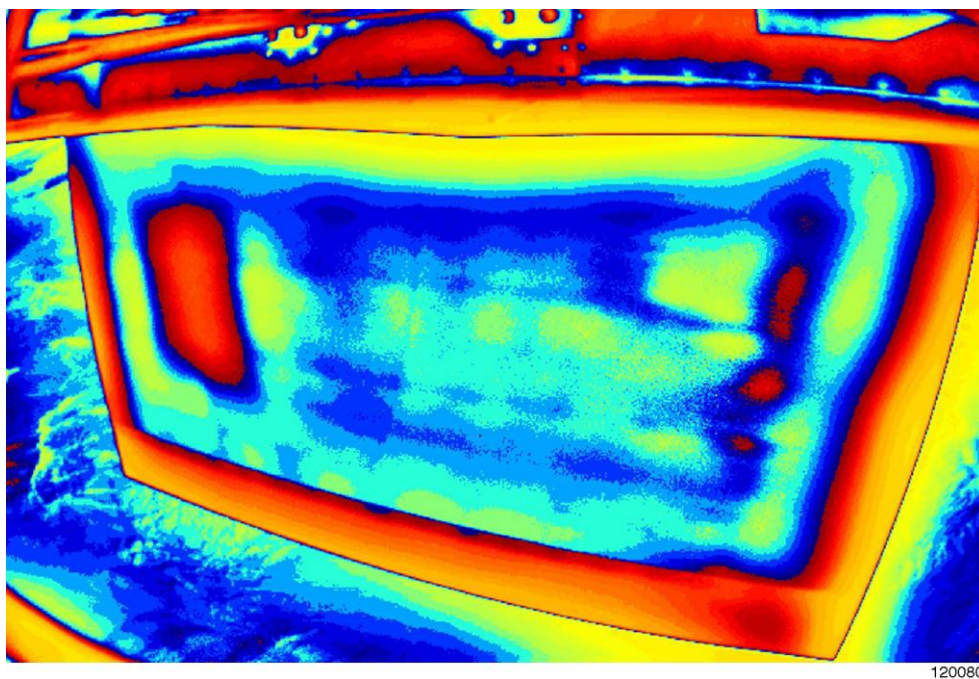
(a) During acceleration.
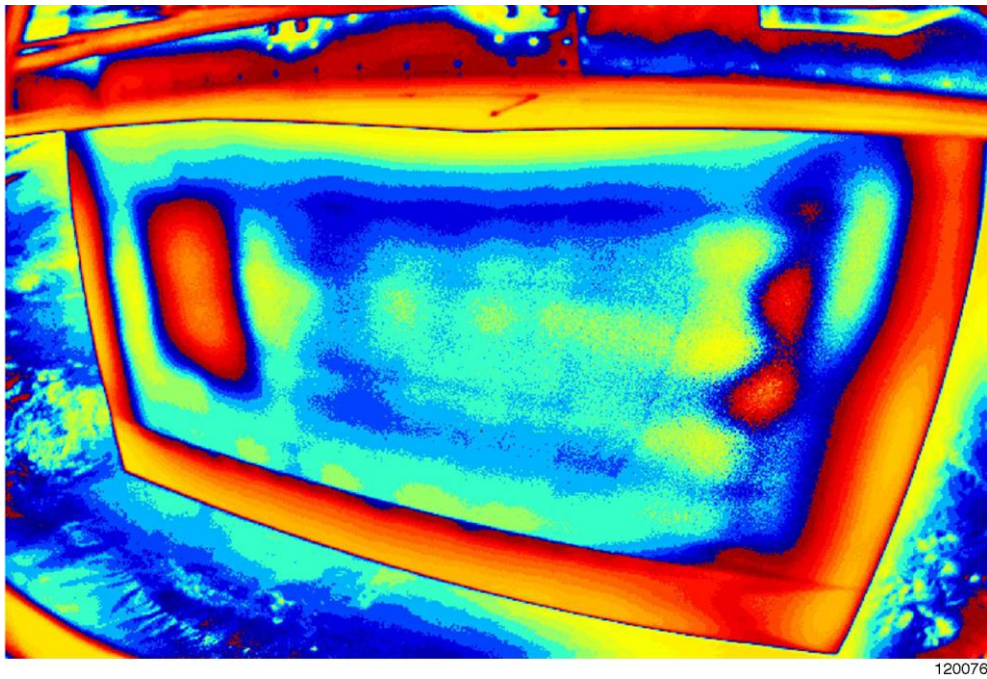
(b) During deceleration.

Figure 10. Processed digital infrared image at M=1.50.

(a) During acceleration.
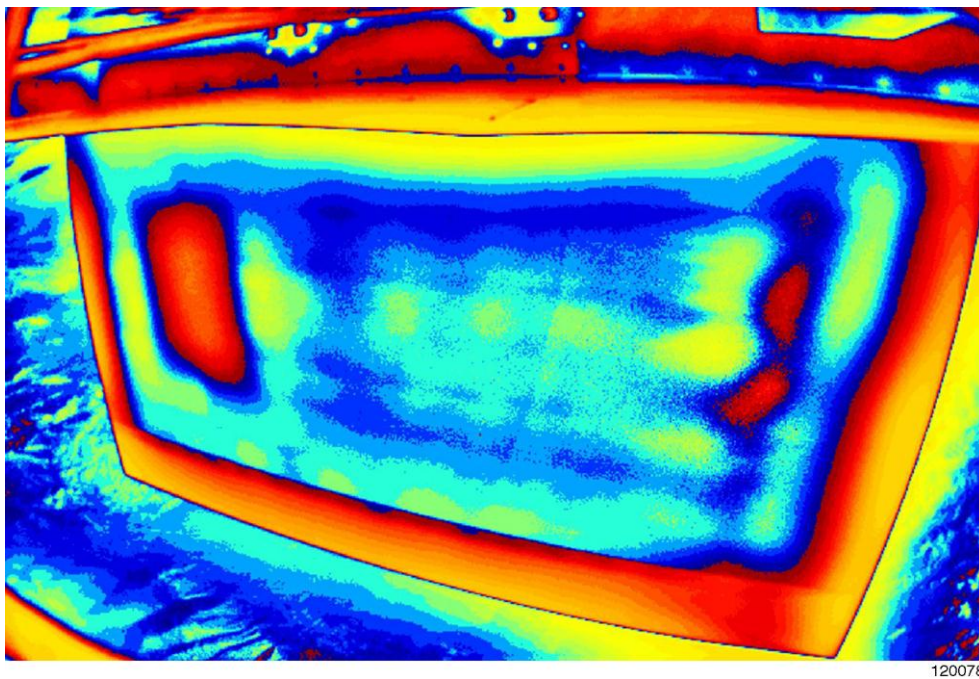
(b) During deceleration.
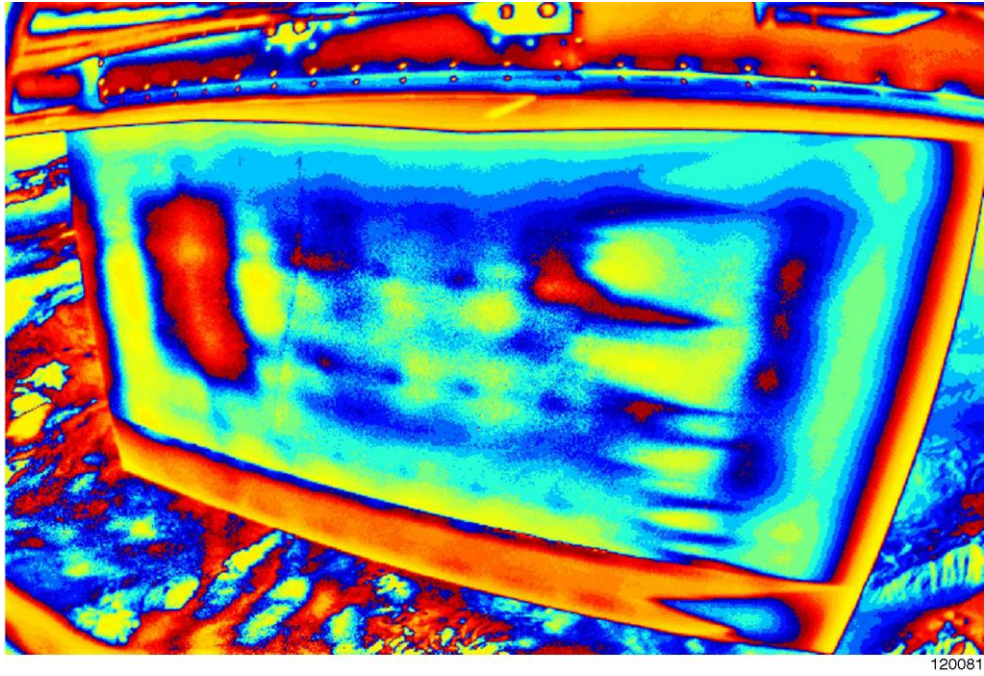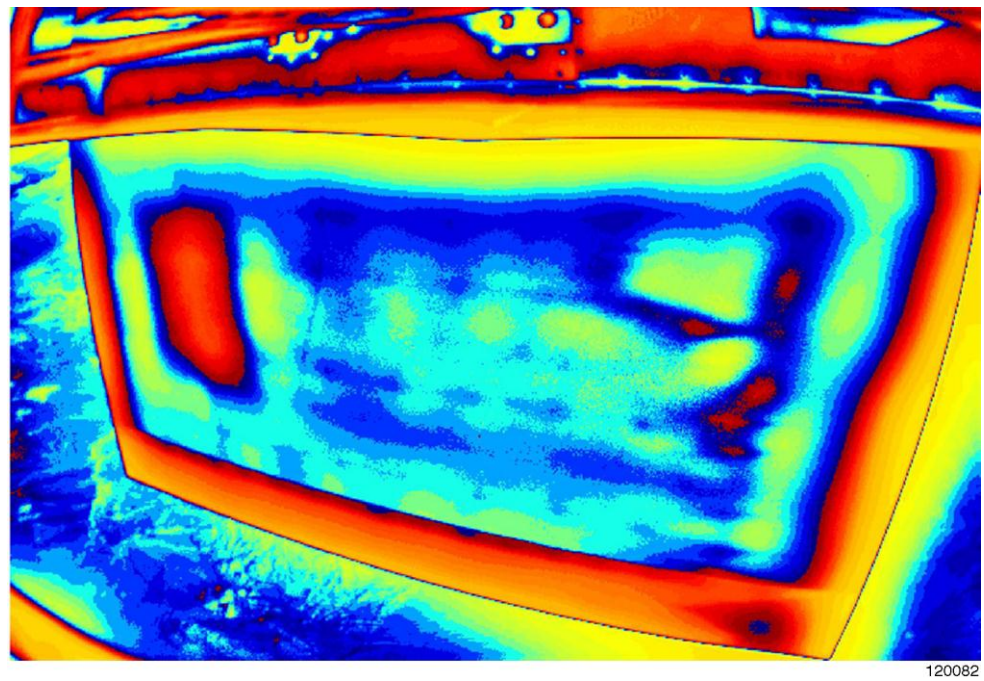
Figure 11. Processed digital infrared image at M=1.60.

(a) During acceleration.

(b) During deceleration.

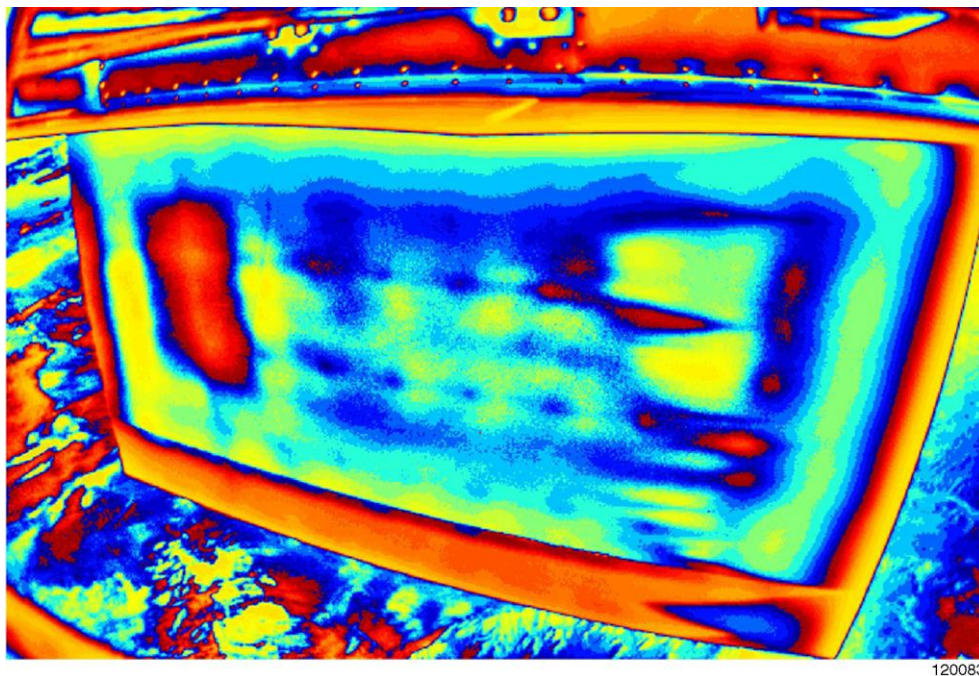Figure 12. Processed digital infrared image at M=1.70.
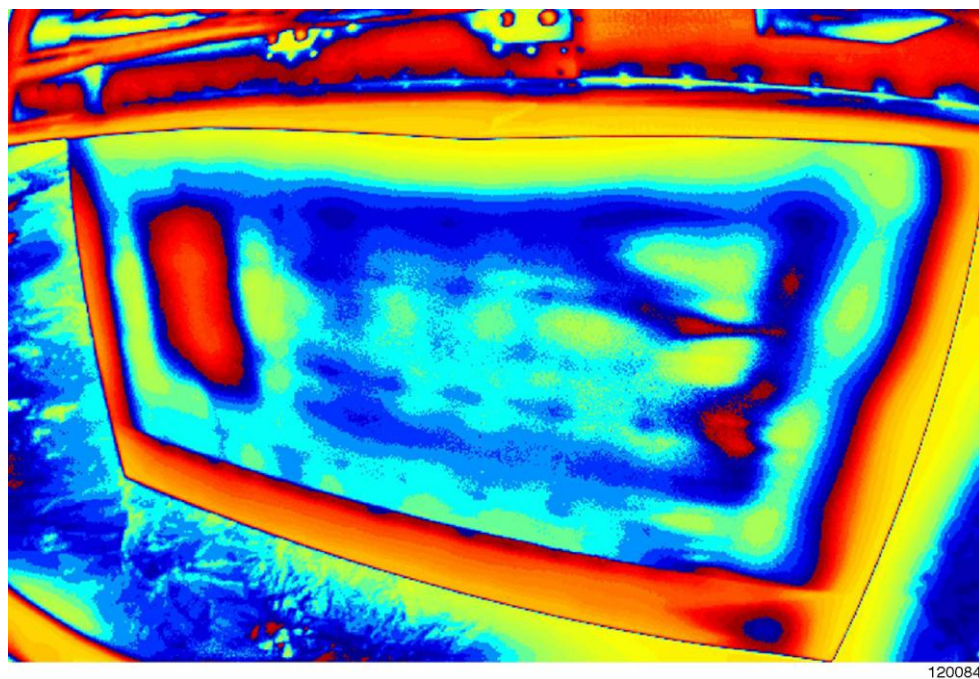
18

(a) During acceleration.

(b) During deceleration.

Figure 13. Processed digital infrared image at M=1.80.

(a) During acceleration.

(b) During deceleration.

Figure 14. Processed digital infrared image at M=1.85.

References

1. Kroo, I., "Unconventional Configurations for Efficient Supersonic Flight," *VKI Lecture Series on Innovative Configurations and Advanced Concepts for Future Civil Aircraft*, 2005.

2. Sturdza, Peter, "An Aerodynamic Design Method for Supersonic Natural Laminar Flow Aircraft," PhD. Thesis, Stanford University, Palo Alto, California, 2003.

3. Chang, Chau-Lyan, *Langley Stability and Transition Analysis Code (LASTRAC) Version 1.2 User Manual*, NASA/TM-2004-213233, 2004.

4. Chang, Chau-Lyan, "LASTRAC.3d: Transition Prediction in 3D Boundary Layers," AIAA Paper 2004-2541, June 2004.

5. Malik, Mujeeb R., *Stability Theory Applications to Laminar-Flow Control*, NASA N90-12513.

6. Joslin, Ronald D., *Overview of Laminar Flow Control*, NASA/TP-1998-208705, 1998.

7. Braslow, Albert L., *A History of Suction-Type Laminar-Flow Control with Emphasis on Flight Research*, NASA Monograph in Aerospace History Number 13, 1999.

8. Chen, Fang-Jeng, Mujeeb R. Malik, and Ivan E. Beckwith, "Advanced Mach 3.5 Axisymmetric Quiet Nozzle," AIAA Paper 90-1592, June 1990.

9. Chen, Fang-Jeng, Mujeeb R. Malik, and Ivan E. Beckwith, "On the Design of a New Mach 3.5 Quiet Nozzle*," Instability and transition; Proceedings of the Workshop, Hampton, VA, May 15-June 9, 1989. Vol. 2 (A91-31301 12-34)*, New York, Springer-Verlag, 1990, pp. 246-257.

10. Beckwith, I.E., F.-J. Chen, and M.R. Malik, *Design and Fabrication Requirements for Low Noise Supersonic/Hypersonic Wind Tunnels*, NASA N90-12555.

11. Banks, D.W., C.P. van Dam, H.J. Shiu, and G.M. Miller, *Visualization of In-Flight Flow Phenomena Using Infrared Thermography*, NASA TM/2000-209027, 2000.

12. Van Dam, C.P., H.J. Shiu, D.W. Banks, R.R. Tracy, and J. Chase, "In-Flight Visualization Of Supersonic Flow Transition Using Infrared Imaging," *Journal of Aircraft*, Vol. 39, No. 6, November-December 2002, pp. 936-944.

13. Reshotko, Eli, "Roughness-Induced Transition Transient Growth in 3-D Supersonic Flow," NATO RTO-EN-AVT-151.

14. Hopkins, Edward J., Don W. Jillie, and Virginia L. Sorensen, *Charts for Estimating Boundary-Layer Transition on Flat Plates,* NASA TN D-5846, 1970.

15. Taylor, John W.R. (editor), *Janes's All the World's Aircraft 1979-1980,* pp. 383-384.